

Magnetic moment of the $\Delta(1232)$ -resonance in chiral effective field theory

Vladimir Pascalutsa* and Marc Vanderhaeghen†

Physics Department, The College of William & Mary, Williamsburg, VA 23187, USA

Theory Group, Jefferson Lab, 12000 Jefferson Ave, Newport News, VA 23606, USA

(Dated: July 15, 2018)

We perform a relativistic chiral effective field theory calculation of the radiative pion photoproduction ($\gamma p \rightarrow \pi^0 p \gamma'$) in the Δ -resonance region, to next-to-leading order in the “delta-expansion”. This work is aimed at a model-independent extraction of the Δ^+ magnetic moment from new precise measurements of this reaction. It also predicts the chiral behavior of Δ 's magnetic moment, which can be used to extrapolate the recent lattice QCD results to the physical point.

PACS numbers: 12.39.Fe, 13.40.Em, 25.20.Dc

The $\Delta(1232)$ -isobar is the most distinguished and well-studied nucleon resonance. However, such a fundamental property as its magnetic dipole moment (MDM) has thusfar escaped a precise determination. The problem is generic to any unstable particle whose lifetime is too short for its MDM to be measurable in the usual way through spin precession experiments. A measurement of the MDM of such an unstable particle can apparently be done only indirectly, in a three-step process, where the particle is first produced, then emits a low-energy photon which plays the role of an external magnetic field, and finally decays. In this way the MDM of Δ^{++} is accessed in the reaction $\pi^+ p \rightarrow \pi^+ p \gamma$ [1, 2] while the MDM of Δ^+ can be determined using the radiative pion photoproduction ($\gamma p \rightarrow \pi^0 p \gamma'$) [3].

A first experiment devoted to the MDM of Δ^+ was completed in 2002 [4]. The value extracted in this experiment, $\mu_{\Delta^+} = 2.7_{-1.3}^{+1.0}(\text{stat.}) \pm 1.5(\text{syst.}) \pm 3(\text{theor.})$ [nuclear magnetons], is based on theoretical input from the phenomenological model [5, 6] of the $\gamma p \rightarrow \pi^0 p \gamma'$ reaction. To improve upon the precision of this measurement, a dedicated series of experiments has recently been carried out by the Crystal Ball Collaboration at MAMI [7]. These experiments achieve about two orders of magnitude better statistics than the pioneering experiment[4]. The aim of the present work is to complement these high-precision measurements with an accurate and model-independent analysis of the $\gamma p \rightarrow \pi^0 p \gamma'$ reaction, within the framework of chiral effective field theory (χ EFT).

The χ EFT of the strong interaction is indispensable, at least at present, in relating the low-energy observables (e.g., hadron masses, magnetic moments, scattering lengths) to *ab initio* QCD calculations on the lattice. On the other hand, χ EFT can and should be used in extracting various hadronic properties from the experiment. In this Letter we will show how χ EFT fulfills both of these roles in a gratifying fashion. The one-loop calculation we present here is sufficient to both complete

the next-to-leading order calculation of the $\gamma p \rightarrow \pi^0 p \gamma'$ reaction, in the Δ -resonance region, and perform a chiral extrapolation of lattice QCD results for Δ 's MDM [8, 9].

Our starting effective Lagrangian is that of the chiral perturbation theory (χ PT) with pion and nucleon fields [10]. The Δ then is included explicitly in the so-called δ -expansion scheme [11]. We organize the Lagrangian $\mathcal{L}^{(i)}$, such that superscript i stands for the power of electromagnetic coupling e plus the number of derivatives of pion and photon fields. Writing here only the terms involving the spin-3/2 isospin-3/2 field ψ^μ of the Δ -isobar gives:¹

$$\begin{aligned} \mathcal{L}_\Delta^{(1)} &= \bar{\psi}_\mu (i\gamma^{\mu\nu\alpha} D_\alpha - M_\Delta \gamma^{\mu\nu}) \psi_\nu \\ &+ \frac{i h_A}{2 f_\pi M_\Delta} \{ \bar{N} T_a \gamma^{\mu\nu\lambda} (\partial_\mu \psi_\nu) D_\lambda \pi^a + \text{H.c.} \} \quad (1a) \\ \mathcal{L}_\Delta^{(2)} &= \frac{ie(\mu_\Delta - 1)}{2M_\Delta} \bar{\psi}_\mu \psi_\nu F^{\mu\nu} \\ &+ \frac{3ieg_M}{2M(M + M_\Delta)} \{ \bar{N} T_3 \partial_\mu \psi_\nu \tilde{F}^{\mu\nu} + \text{H.c.} \} \\ &- \frac{eh_A}{2f_\pi M_\Delta} \{ \bar{N} T_a \gamma^{\mu\nu\lambda} A_\mu \psi_\nu \partial_\lambda \pi^a + \text{H.c.} \} \quad (1b) \\ \mathcal{L}_\Delta^{(3)} &= \frac{-3eg_E}{2M(M + M_\Delta)} \{ \bar{N} T_3 \gamma_5 \partial_\mu \psi_\nu F^{\mu\nu} + \text{H.c.} \} \quad (1c) \end{aligned}$$

where M and M_Δ are, respectively, the nucleon and Δ -isobar masses, N and π^a ($a = 1, 2, 3$) stand for the nucleon and pion fields, D_μ is the covariant derivative ensuring the electromagnetic gauge-invariance, $F^{\mu\nu}$ and $\tilde{F}^{\mu\nu}$ are the electromagnetic field strength and its dual, T_a are the isospin 1/2 to 3/2 transition matrices, coupling constants $f_\pi = 92.4$ MeV, $g_M = 2.94$, $g_E = -0.96$, see [11, 12] for further details. The MDM μ_Δ is defined

¹ Here we introduce totally antisymmetric products of γ -matrices: $\gamma^{\mu\nu} = \frac{1}{2}[\gamma^\mu, \gamma^\nu]$, $\gamma^{\mu\nu\alpha} = \frac{1}{2}\{\gamma^{\mu\nu}, \gamma^\alpha\} = i\varepsilon^{\mu\nu\alpha\beta}\gamma_\beta\gamma_5$.

here in units of $[e/2M_\Delta]$. We omit the higher electromagnetic moments, because they do not contribute at the orders that we consider.

Note that $\mathcal{L}_\Delta^{(1)}$ contains the free Lagrangian, which is formulated in [13] such that the number of spin degrees of freedom of the relativistic spin-3/2 field is constrained to the physical number: $2s + 1 = 4$. The N to Δ transition couplings in Eq. (1) are consistent with these constraints [14, 15]. The $\gamma\Delta\Delta$ coupling is more subtle since in this case constraints do not hold for sufficiently strong electromagnetic fields, see, e.g., [16]. We do not deal with this problem here, thus assuming the electromagnetic field to be weak, compared to the Δ mass scale.

We now briefly describe the power counting in the δ -expansion scheme. The excitation energy of the Δ -resonance, i.e., $\Delta \equiv M_\Delta - M_N \simeq 293$ MeV is treated as a light scale, so $\Delta \ll \Lambda$, where $\Lambda \sim 1$ GeV stands for the heavy scales of the theory. At the same time, Δ is counted differently from the other light scale of the theory – the pion mass, m_π . Namely, Δ/Λ counts as one power of the small parameter δ while m_π/Λ counts as two powers of δ . Each graph can then be characterized by an overall δ -counting index n , which simply tells us that the graph is of size δ^n . Because the theory has two distinct light scales (m_π and Δ) the δ -counting index depends on whether the characteristic momentum p is in the low-energy region ($p \sim m_\pi$) or in the resonance region ($p \sim \Delta$). In the low-energy region the index of a graph with L loops, N_π pion propagators, N_N nucleon propagators, N_Δ Δ -isobar propagators, and V_i vertices of dimension i is $n = 2n_{\chi PT} - N_\Delta$, where $n_{\chi PT} = \sum_i iV_i + 4L - N_N - 2N_\pi$ is the index in χPT with no Δ 's [10].

In the resonance region, one needs to distinguish the one- Δ -reducible (O Δ R) graphs, because they contain Δ propagators which go as $1/(p - \Delta)$ and hence such graphs are large and all need to be included. Their resummation amounts to dressing the Δ propagators so that they behave as $1/(p - \Delta - \Sigma)$. The self-energy Σ begins at order p^3 and thus, for $p \sim \Delta$, the dressed O Δ R propagator goes as $1/\delta^3$. If the number of such propagators in a graph is $N_{O\Delta R}$, the power-counting index of this graph in the resonance region is given by $n = n_{\chi PT} - N_\Delta - 2N_{O\Delta R}$.

Consider now the amplitude for the $\gamma p \rightarrow \pi^0 p \gamma'$ reaction. The optimal sensitivity to the MDM term is achieved when the incident photon energy is in the vicinity of Δ , while the outgoing photon energy is of order of m_π . In this case the $\gamma p \rightarrow \pi^0 p \gamma'$ amplitude to next-to-leading order (NLO) in the δ -expansion is given by the diagrams 1(a), (b), and (c), where the shaded blobs, in addition to vertices from Eq. (1), contain the one-loop corrections shown in Fig. 1(d), (e), (f). To present our calculation of the loops we introduce the mass ratios:

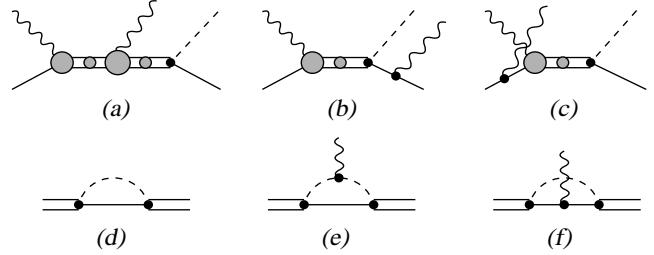


FIG. 1: Diagrams for the $\gamma p \rightarrow \pi^0 p \gamma'$ reaction at NLO in the δ -expansion, considered in this work. Double lines represent the Δ propagators.

$\mu = m_\pi/M_\Delta$, $r = M/M_\Delta$. The self-energy, Fig. 1(d), has the following form

$$\Sigma^{\mu\nu}(p) = A(p^2)\gamma^{\mu\nu\alpha} p_\alpha + B(p^2)\gamma^{\mu\nu}, \quad (2a)$$

where the scalar functions, after dimensional regularization, take the form

$$A(p^2) = -\frac{1}{2}C^2 \int_0^1 dx x \mathcal{M}^2 (L - 1 + \ln \mathcal{M}^2), \quad (2b)$$

$$B(p^2) = -\frac{1}{2}C^2 r \int_0^1 dx \mathcal{M}^2 (L - 1 + \ln \mathcal{M}^2), \quad (2c)$$

with $C = h_A M_\Delta / (8\pi f_\pi)$, $L = -2/(4 - d) + \gamma_E + \ln(4\pi M_\Delta/\Lambda)$, $d \rightarrow 4$ the number of dimensions, $\gamma_E = -\Gamma'(1) \simeq 0.5772$, Λ the renormalization scale and

$$\mathcal{M}^2(x) = x\mu^2 + (1 - x)r^2 - x(1 - x)(p^2/M_\Delta^2) - i\epsilon. \quad (3)$$

After the on-mass-shell wave-function and mass renormalizations the NLO Δ -propagator is given by

$$S_{\mu\nu}(p) = \frac{-\mathcal{P}_{\mu\nu}^{(3/2)}(p)}{(p - M_\Delta)[1 - i\text{Im} \Sigma'(M_\Delta)] - i\text{Im} \Sigma(M_\Delta)}, \quad (4)$$

where we have introduced the spin-3/2 projection operator, $\mathcal{P}^{(3/2)}$, and the following definitions: $\Sigma(M_\Delta) = M_\Delta A(M_\Delta^2) + B(M_\Delta^2)$, $\Sigma'(M_\Delta) = A(M_\Delta^2) + 2M_\Delta(\partial/\partial p^2)[M_\Delta A(p^2) + B(p^2)]_{p^2=M_\Delta^2}$. These functions are complex when the Δ -isobar is heavier than the pion production threshold, $M_\Delta > M + m_\pi$. In this case $\mathcal{M}^2 < 0$ and hence the logarithm in Eq. (2) gives rise to an imaginary part:

$$\text{Im} \Sigma(M_\Delta) = -(2\pi/3)M_\Delta C^2(\alpha + r)\lambda^3, \quad (5a)$$

$$\begin{aligned} \text{Im} \Sigma'(M_\Delta) &= -2\pi C^2 \lambda [\alpha(1 - \alpha)(\alpha + r) \\ &\quad - \frac{1}{3}\lambda^2(r + r^2 - \mu^2)], \end{aligned} \quad (5b)$$

with $\alpha = \frac{1}{2}(1 + r^2 - \mu^2)$, $\lambda = \sqrt{\alpha^2 - r^2}$. We note that the width of the resonance is given by $\Gamma_\Delta = -2\text{Im} \Sigma(M_\Delta)$, and find that the experimental value $\Gamma_\Delta \simeq 115$ MeV

translates into $h_A \simeq 2.85$, the value which we shall use in the numerical calculations.

The $\gamma\Delta\Delta$ vertex, omitting the electric quadrupole and magnetic octupole terms, is written in the form:

$$\begin{aligned} & \bar{u}_\alpha(p') \Gamma^{\mu\alpha\beta}(p', p) u_\beta(p) \varepsilon_\mu \\ &= e \bar{u}_\alpha(p') \left[\not{\varepsilon} F(q^2) + \frac{(p' + p) \cdot \varepsilon}{2M_\Delta} G(q^2) \right] u^\alpha(p), \end{aligned} \quad (6)$$

where ε^μ is the photon polarization vector, u^α is the vector-spinor of the Δ . In this notation, the MDM is given by $\mu_\Delta = F(0)$. The Ward-Takahashi identity,

$$q_\mu \Gamma^{\mu\alpha\beta}(p', p) = e \left[(S^{-1})^{\alpha\beta}(p') - (S^{-1})^{\alpha\beta}(p) \right], \quad (7)$$

demands that $F(0) + G(0) = 1 - \Sigma'(M_\Delta)$. This condition is verified explicitly in our calculation. Since we have already given the expression for the self-energy, we present here only the expressions for G . The contributions of diagrams 1(e) and 1(f), at $q^2 = 0$, are:

$$\begin{aligned} G^{(e)}(0) &= -C^2 \int_0^1 dx x(1-2x)(x-r) \\ &\quad \times \{L + \ln[x\mu^2 + (1-x)r^2 - x(1-x) - i\epsilon]\}, \quad (8) \\ G^{(f)}(0) &= -2C^2 \int_0^1 dx x^2(1-x-r) \\ &\quad \times \{L + \ln[xr^2 + (1-x)\mu^2 - x(1-x) - i\epsilon]\}. \quad (9) \end{aligned}$$

Their contribution to μ_Δ for different isospin states is, e.g., $\mu_{\Delta^{++}}^{(loop)} = F^{(e)} + F^{(f)}$, $\mu_{\Delta^+}^{(loop)} = (1/3)F^{(e)} + (2/3)F^{(f)}$.

As all lattice data for μ_Δ at present and in the foreseeable future are for larger than the physical values of m_π , their comparison with experiment requires the knowledge of the m_π -dependence for this quantity. In contrast to the heavy-baryon result [17], our χ EFT calculation is manifestly relativistic, and, as argued earlier for the nucleon [18], should be better suited for such extrapolations of lattice data. Figure 2 shows the pion mass dependence of real and imaginary parts of the Δ^+ and Δ^{++} MDMs, according to our one-loop calculation. Each of the two solid curves has a free parameter, the counterterm μ_Δ from $\mathcal{L}_\Delta^{(2)}$, adjusted to agree with the lattice data at larger values of m_π . As can be seen from Fig. 2, the Δ MDM develops an imaginary part when $m_\pi < \Delta = M_\Delta - M$, whereas the real part has a pronounced cusp at $m_\pi = \Delta$. For μ_{Δ^+} our curve is in disagreement with the trend of the recent lattice data, which possibly is due to the ‘‘quenching’’ in the lattice calculations. The dotted line in Fig. 2 shows the result [18] for the magnetic moment for the proton. One sees that μ_{Δ^+} and μ_p , while having very distinct behavior for small m_π , are approximately equal for larger values of m_π .

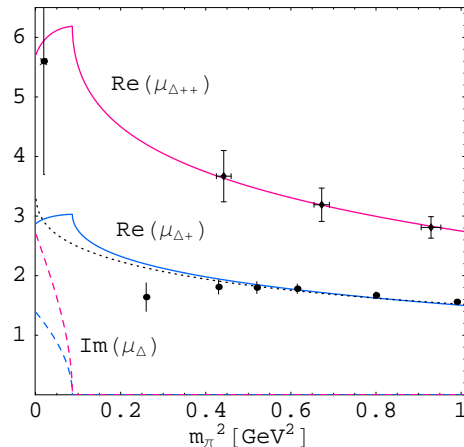


FIG. 2: Pion mass dependence of the real (solid curves) and imaginary (dashed curves) parts of Δ^{++} and Δ^+ MDMs [in nuclear magnetons]. Dotted curve is the result for the proton magnetic moment from Ref. [18]. The experimental data point for Δ^{++} is from PDG analysis [19]. Lattice data are from [8] for Δ^{++} and from [9] for Δ^+ .

We next discuss our results for the $\gamma p \rightarrow \pi^0 p \gamma'$ observables. The NLO calculation of this process in the δ -expansion corresponds with the diagrams of Fig. 1. As outlined above, this calculation completely fixes the imaginary part of the $\gamma\Delta\Delta$ vertex. It leaves μ_Δ as only free parameter, which enters as a low energy constant in $\mathcal{L}^{(2)}$. Thus the real part of μ_{Δ^+} is to be extracted from the $\gamma p \rightarrow \pi^0 p \gamma'$ observables, some of which are shown in Fig. 3 for an incoming photon energy $E_\gamma^{lab} = 400$ MeV as function of the emitted photon energy $E_\gamma^{c.m.}$. In the soft-photon limit ($E_\gamma^{c.m.} \rightarrow 0$), the $\gamma p \rightarrow \pi^0 p \gamma'$ reaction is completely determined from the bremsstrahlung process from the initial and final protons. The deviations of the $\gamma p \rightarrow \pi^0 p \gamma'$ observables, away from the soft-photon limit, will then allow to study the sensitivity to μ_{Δ^+} . It is therefore very useful to introduce the ratio [6]:

$$R \equiv \frac{1}{\sigma_\pi} \cdot E_\gamma' \frac{d\sigma}{dE_\gamma'}, \quad (10)$$

where $d\sigma/dE_\gamma'$ is the $\gamma p \rightarrow \pi^0 p \gamma'$ cross section integrated over the pion and photon angles, and σ_π is the angular integrated cross section for the $\gamma p \rightarrow \pi^0 p$ process weighted with the bremsstrahlung factor, as detailed in [6]. This ratio R has the property that in the soft-photon limit, the low energy theorem predicts that $R \rightarrow 1$. From Fig. 3 one then sees that the EFT calculation obeys this theorem. This is a consequence of gauge-invariance which is maintained exactly throughout our calculation, also away from the soft-photon limit.

The EFT result for R shows clear deviations from unity at higher outgoing photon energies, in good agreement

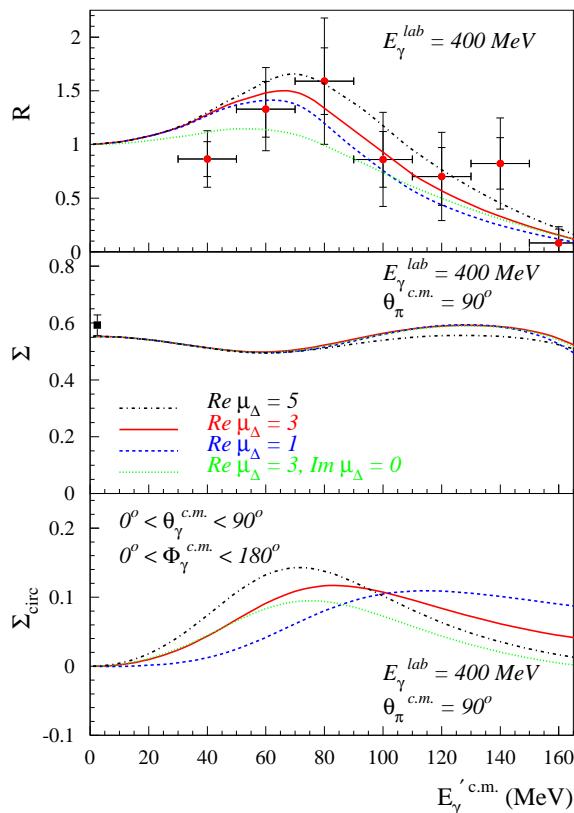


FIG. 3: The outgoing photon energy dependence of the $\gamma p \rightarrow \pi^0 p \gamma'$ observables for different values of μ_{Δ^+} (in units $e/2M_{\Delta}$). Top panel: the ratio of $\gamma p \rightarrow \pi^0 p \gamma'$ to $\gamma p \rightarrow \pi^0 p$ cross-sections Eq. (10). Data points are from [4]. Middle panel: the linear-polarization photon asymmetry of the $\gamma p \rightarrow \pi^0 p \gamma'$ cross-sections differential w.r.t. the outgoing photon energy and pion c.m. angle. The data point at $E'_\gamma = 0$ corresponds with the $\gamma p \rightarrow \pi^0 p$ photon asymmetry from [20]. Lower panel: the circular-polarization photon asymmetry (as defined in [6]), where the outgoing photon angles have been integrated over the indicated range.

with the first data for this process [4]. The sensitivity of the EFT calculation to the μ_{Δ} is a very promising setting for the dedicated second-generation experiment which has recently been completed by the Crystal Ball Coll. at MAMI [7]. It improves upon the statistics of the first experiment (Fig. 3) by at least two orders of magnitude and will allow for a reliable extraction of μ_{Δ^+} using the EFT calculation presented here.

Besides the cross section, the $\gamma p \rightarrow \pi^0 p \gamma'$ asymmetries for linearly and circularly polarized incident photons have also been measured in the recent dedicated experiment [7]. They are also shown in Fig. 3. The photon asymmetry for linearly polarized photons, Σ , at $E'_\gamma = 0$ exactly reduces to the $\gamma p \rightarrow \pi^0 p$ asymmetry. It

is seen from Fig. 3 that our calculation is in good agreement with the experimental value. At higher outgoing photon energies, the photon asymmetry as predicted by the NLO EFT calculation remains nearly constant and is very weakly dependent on μ_{Δ} . It is an ideal observable for a consistency check of the EFT calculation and to test that the Δ diagrams of Fig. 1 indeed dominate the process. Mechanisms involving π -photoproduction Born terms followed by πN rescattering have been considered in model calculations [5, 6]. In the δ -counting they start contributing at next-next-to-leading order and therefore will provide the main source of corrections to the present NLO results.

The asymmetry for circularly polarized photons, Σ_{circ} , (which is exactly zero for a two body process due to reflection symmetry w.r.t. the reaction plane) has been proposed [6] as a unique observable to enhance the sensitivity to μ_{Δ} . Indeed, in the soft-photon limit, where the $\gamma p \rightarrow \pi^0 p \gamma'$ process reduces to a two-body process, Σ_{circ} is exactly zero. Therefore, its value at higher outgoing photon energies is directly proportional to μ_{Δ} . One sees from Fig. 3 (lower panel) that our EFT calculation supports this observation, and shows sizeably different asymmetries for different values of μ_{Δ} . A combined fit of all three observables shown in Fig. 3 will therefore allow for a very stringent test of the EFT calculation, which can then be used to extract the Δ^+ MDM.

In conclusion, we have performed a manifestly gauge- and Lorentz-invariant chiral EFT calculation for the $\gamma p \rightarrow \pi^0 p \gamma'$ reaction in the $\Delta(1232)$ resonance region. To next-to-leading order in the δ -expansion, the only free parameter entering the calculation is the Δ^+ magnetic dipole moment μ_{Δ^+} . Due to the unstable nature of the Δ -isobar its magnetic moment acquires an imaginary part, an effect which is computed in this work and will be taken into account in the extraction of μ_{Δ} from experiment. Our present calculation is found to be in good agreement with first experimental results for the $\gamma p \rightarrow \pi^0 p \gamma'$ cross sections, and will allow for a model-independent extraction of μ_{Δ^+} from a combined fit to cross sections and photon asymmetries measured in new dedicated experiments. At the same time, this chiral EFT calculation provides a crucial connection of present lattice QCD results for μ_{Δ} at values of $m_\pi > M_{\Delta} - M$ to the physical pion mass.

We thank Barry Holstein for interesting discussions. This work is supported in part by DOE grant no. DE-FG02-04ER41302 and contract DE-AC05-84ER-40150 under which SURA operates the Jefferson Laboratory.

* Electronic address: vlad@jlab.org

† Electronic address: marcvdh@jlab.org

- [1] B.M.K. Nefkens *et al.*, Phys. Rev. D **18**, 3911 (1978).
- [2] A. Bosshard *et al.*, Phys. Rev. D **44**, 1962 (1991).
- [3] D. Drechsel, M. Vanderhaeghen, M. M. Giannini and E. Santopinto, Phys. Lett. B **484**, 236 (2000).
- [4] M. Kotulla *et al.*, Phys. Rev. Lett. **89**, 272001 (2002).
- [5] D. Drechsel and M. Vanderhaeghen, Phys. Rev. C **64**, 065202 (2001).
- [6] W. T. Chiang, M. Vanderhaeghen, S. N. Yang and D. Drechsel, Phys. Rev. C **71**, 015204 (2005).
- [7] R. Beck, B. Nefkens, spokespersons Crystal Ball @ MAMI experiment.
- [8] D. B. Leinweber, T. Draper, and R. M. Woloshyn, Phys. Rev. D **46**, 3067 (1992); I. C. Cloet, D. B. Leinweber and A. W. Thomas, Phys. Lett. B **563**, 157 (2003).
- [9] F. X. Lee, R. Kelly, L. Zhou and W. Wilcox, arXiv:hep-lat/0410037.
- [10] J. Gasser, M. E. Sainio and A. Svarc, Nucl. Phys. B **307**, 779 (1988).
- [11] V. Pascalutsa and D. R. Phillips, Phys. Rev. C **67**, 055202 (2003).
- [12] V. Pascalutsa and D. R. Phillips, *ibid.* **68**, 055205 (2003).
- [13] W. Rarita and J. S. Schwinger, Phys. Rev. **60**, 61 (1941).
- [14] V. Pascalutsa, Phys. Rev. D **58**, 096002 (1998).
- [15] V. Pascalutsa and R. Timmermans, Phys. Rev. C **60**, 042201 (1999).
- [16] S. Deser, V. Pascalutsa and A. Waldron, Phys. Rev. D **62**, 105031 (2000).
- [17] M. N. Butler, M. J. Savage and R. P. Springer, Phys. Rev. D **49**, 3459 (1994); M. K. Banerjee and J. Milana, *ibid.* **54**, 5804 (1996).
- [18] V. Pascalutsa, B. R. Holstein and M. Vanderhaeghen, Phys. Lett. B **600**, 239 (2004).
- [19] K. Hagiwara *et al.* (Particle Data Group), Phys. Rev. D **66**, 010001 (2002).
- [20] R. Beck *et al.*, Phys. Rev. Lett. **78**, 606 (1997); Phys. Rev. C **61**, 035204 (2000).